Phenomenological model to fit complex permittivity data of water from radio to optical frequencies

Fridon Shubitidze and Ulf Österberg
Thayer School of Engineering, Dartmouth College, Hanover, New Hampshire 03755-8000, USA
(Received 26 September 2006; revised manuscript received 22 December 2006; published 25 April 2007)

A general factorized form of the dielectric function together with a fractional model-based parameter estimation method is used to provide an accurate analytical formula for the complex refractive index in water for the frequency range 10^8–10^{16} Hz. The analytical formula is derived using a combination of a microscopic frequency-dependent rational function for adjusting zeros and poles of the dielectric dispersion together with the macroscopic statistical Fermi-Dirac distribution to provide a description of both the real and imaginary parts of the complex permittivity for water. The Fermi-Dirac distribution allows us to model the dramatic reduction in the imaginary part of the permittivity in the visible window of the water spectrum.

DOI: 10.1103/PhysRevE.75.046608 PACS number(s): 42.25.Bs, 42.65.An

I. INTRODUCTION

Water is an important medium for many electromagnetic applications—e.g., medical imaging and atmospheric and underwater communication. It is therefore not surprising that many measurements exist of the refractive index of water as a function of wavelength [1]. For many practical applications these "look-up tables" for the refractive index are sufficient; however, for other purposes they are not. Two examples, which each require an explicit analytic formula for the wavelength-dependent refractive index of water, are the calculation of van der Waals interactions and the modeling of transient pulse propagation. The van der Waals force is used to calculate interactions between dielectrics when these are separated by water, such as those in colloidal systems [2]. The other example, involving precursor propagation in water [3–10], uses the refractive index in conjunction with the powerful methods of asymptotic analysis in the frequency domain [11] and wave propagator analysis in the time domain [12] to carefully and accurately analyze the creation and evolution of transient pulse propagation. Nevertheless, despite recent progress, there is no good analytical model which accurately describes the wavelength-dependent complex refractive index in water [3,7,13,14]. The majority of the existing models use linear combinations of Debye (or Rocard-Powles) and Lorentz resonances [3,7,13]. Although these representations do a good job of describing the real part of the refractive index over large frequency intervals, they are much less accurate in describing the imaginary part for frequencies above 1 THz. A possible reason for the poor fit to data for higher frequencies could be the lack of interaction terms because the polarized Debye dipoles and the Lorentz harmonic oscillators are only *added* to each other [15–17]. The Diaz-Alexopoulos model [14] is more successful in describing the imaginary part of the refractive index using a generalized fractional form of the dielectric permittivity. This approach was first introduced by Berreman and Unterwald [18] to describe reststrahlen reflectance data from solids. The significance of the fractional form is that it allows modeling of molecular interactions and anharmonic oscillators. Because of its makeup,

$$\varepsilon = \frac{\prod_{m=1}^{M} (\omega - Z_m)}{\prod_{n=1}^{N} (\omega - P_n)}, \tag{1}$$

it automatically fulfills the necessary causality conditions and by restricting $M < N-1$ it also decreases with wavelength for higher frequencies in accordance with observations. The position of the zeros (Z_m) and poles (P_n) can be used to address phonon interactions, vibrations, and resonances [19]. The Rocard-Powles, which is the first-order correction to the Debye model, has some of the fractional form features but it does not have enough independent parameters to allow for fitting to data over a large frequency interval. Following Diaz and Alexopoulos, one can use the analogy between electric circuits and a linear dielectric [20] to fit Eq. (1) to published measured data for water [21]. This approach captures the dramatic reduction in absorption for water in the visible regime better than any other model; however, it is still one to two orders of magnitude off for many frequencies.

The approach we have taken builds on the success by Diaz and Alexopoulos [14] and uses a fractional form for the dielectric permittivity. Compared with Diaz and Alexopoulos we provide a formula of the real part of the complex permittivity as well as a better description of the imaginary part of the complex permittivity in the visible window of the water spectrum, region 2 in Fig. 1. We do this by extending the Diaz-Alexopoulos rational function approach in two ways: we use more products in our rational function expansion and we relate the poles to experimentally observed vibrational and electronic resonances in water. Second, we use the Fermi-Dirac distribution to model the reduced density of states in region 2. The kinetic and potential energy terms in the Fermi-Dirac distribution we obtain from a study by Toukan and Rahman [22] where they use a flexible rotating water molecule for calculating the kinetic part and an experimentally verified Lennard-Jones potential for calculating the potential energy. Our model is a first attempt to provide a comprehensive analytic formula for the complex permittivity

in water for use in theoretical calculations over large frequency regions.

II. DERIVATION OF A FITTING ALGORITHM FOR THE COMPLEX PERMITTIVITY OF WATER

It may seem strange that a "simple" medium such as water could cause so many problems to model. The water molecule itself is relatively simple with two hydrogen atoms covalently bonded to an oxygen atom. What is believed to make liquid water so complex is the variable density of hydrogen bonding that connects the different water molecules to each other, producing a dynamic entity [15]. In addition, the chemical nature of a single hydrogen bond in water is incompletely understood. The hydrogen bond is 10–20 times weaker than the covalent bond [16], placing it closer in strength to van der Waals bonds. The issue of how much of the hydrogen bond is covalent versus electrostatic in character is a difficult one and is still under investigation for *ab initio* modeling optical absorption in water [17]. Our approach avoids many of the difficulties associated with *ab initio* calculations by averaging over large a volume of water clusters. We use a volume of 10^{-9} m^3 which consists of approximately 10^{20} water molecules. Since our main concern is transient pulse propagation we use a volume that is based on the physical size of a 100-fs laser pulse with a 5-mm radius at 800 nm [10].

Most fitting routines related to electromagnetic problems work in either the time or frequency domain for which generic descriptions are given by exponentials and pole series, respectively [23]. Due to the large database of absorption as a function of wavelength for water [1], we will mostly focus on the frequency domain using the pole series approach for representing the refractive index of water between 10^8 and 10^{16} Hz. The frequency interval was chosen solely based on available measured data.

Our fitting routine is based on the usual expression for the complex refractive index $n(\omega)$,

$$n(\omega) = n_r(\omega) + in_i(\omega). \tag{2}$$

For our extended analysis, we introduce the two complex functions $a(\omega)$ and $b(\omega)$, such that

$$n_r(\omega) = \mathrm{Re}[a(\omega)]\mathrm{Re}[b(\omega)], \tag{3}$$

$$n_i(\omega) = \mathrm{Im}[a(\omega)]\mathrm{Im}[b(\omega)]. \tag{4}$$

The functions $a(\omega)$ and $b(\omega)$ are associated with microscopic and macroscopic physical phenomena, respectively. $a(\omega)$ is divided into two parts, a resonant and a nonresonant part,

$$a_j(\omega) = a_{j,res}(\omega) + a_{j,nres}(\omega), \tag{5}$$

where j refers to a particular resonance. The resonant part of the $a(\omega)$ function in Eq. (5) can be expanded into a rational function, where the power of the denominator polynomial is larger or equal to that of the numerator,

$$a_{j,res}(\omega) = \sum_{m=1}^{M} \frac{R_{j,m}}{\omega - \omega_{j,m}}, \tag{6}$$

where $\omega_{j,m}$ is a complex resonance. The nonresonance part can be expanded in terms of the complex frequencies ω between powers 0 to P,

$$a_{nres}(\omega) = \sum_{p=0}^{P} C_{j,p}\omega^p. \tag{7}$$

The nonresonant part accounts for the frequency regions outside of the resonances. Combining the resonant and nonresonant terms into a least-common-denominator form we obtain a rational function representation of $a(\omega)$ based on the rational fitting model by Miller [23],

$$a(\omega) = \sum_{i=1}^{M} \frac{N_j(\omega)}{D_j(\omega)}, \tag{8}$$

where

$$N_j(\omega) = \sum_{\ell=0}^{n_j} N_j^\ell \omega^\ell, \quad D_j(\omega) = \sum_{\ell=0}^{d_j} D_j^\ell \omega^\ell. \tag{9}$$

Coefficients N_j^ℓ and D_j^ℓ are unknowns. To obtain these coefficients, we fit against the measured data as tabulated by Segelstein [21]. The previously introduced coefficients $R_{j,m}$ and $C_{j,p}$ in Eqs. (6) and (7) have been absorbed into the new fitting coefficients N_j^ℓ and D_j^ℓ. The physical significance of $a(\omega)$ is similar to the general dispersion relation by Berreman and Unterwald with the addition of the double sum which we use to center the ℓ sums around eight major resonances of the water spectrum in Fig. 3 and Table I in the next section.

It should be possible to use the pole-zero series of the function $a(\omega)$ to obtain a fit to existing water data. However, we found that, using only the $a(\omega)$ function, we could never fit the eight orders of magnitude decrease in the imaginary part of the refractive index in the visible window better than in the work by Diaz and Alexopoulos [14]. To circumvent this difficulty we approach the visible window as if it is a band gap with dramatically reduced density of states. The function $b(\omega)$ was introduced to provide a method to model the visible window using a statistical approach. $b(\omega)$ can be expressed as

$$b(\omega) = D(\omega) + L(\omega), \tag{10}$$

where $D(\omega)$ and $L(\omega)$ are based on classical Debye one-pole and Lorentz double-pole relaxation models multiplied by the Fermi-Dirac distribution $F(\omega)$, respectively,

$$D(\omega) = \sqrt{\chi_0\left[1 - \frac{1}{\ln\ln(\tau_2/\tau_1)}\right]}\ln\frac{i\omega\tau_2 + 1}{i\omega\tau_1 + 1}F(\omega), \tag{11}$$

$$L(\omega) = \sqrt{\varepsilon_\infty - \frac{\omega_0^2(\varepsilon_s - \varepsilon_\infty)}{\omega^2 - 2i\gamma\omega - \omega_0^2} F(\omega)}. \tag{12}$$

χ_0 and ε_∞ are the low- and high-frequency responses for the Debye and Lorentz distributions, respectively. $F(\omega)$ is defined as

$$F(\omega) = \frac{1}{1 + e^{\hbar\omega/(3/2kT) - E_p}}, \tag{13}$$

$\hbar = 1.062 \times 10^{-34}$ [J/Hz] Plank's constant, E_p is the potential energy, $k = 1.38 \times 10^{-23}$ [J/K], and T is the temperature in degrees kelvin. In reference to Fig. 1, we used the Debye term to provide the general structure to region 1 which is characterized by the molecular polarizability of the water molecules and their rotational and vibrational resonances. In a similar manner we used, the Lorentz term to describe the general electronic resonance behavior of region 3. Region 2 is the difficult region to model. Even though the reduced absorption in region 2 suggests a lack of either Debye or Lorentz interactions, we know, e.g., that the resonant peaks in region 2*A* are all due to vibrational overtones lending themselves to a Debye description [24] and the increase in absorption in region 2*B* is mostly due to increased electronic transitions [25]. So recognizing that both vibrational and electronic interactions are occurring in region 2, but with reduced overall effect, we use the idea behind the Lindhard equation for an electron gas [26]. We multiply the refractive index parts by the Fermi-Dirac distribution to compensate for the drastically reduced density of states in the visible window region. To describe the potential energy E_p, we use the expression derived by Toukan and Rahman [22],

$$E_p = V_{\text{O-O}} + V_{\text{O-H}} + V_{\text{H-H}}, \tag{14}$$

where the subscripts indicate the atoms responsible for the potentials. For the intermolecular interactions, $V_{\text{O-O}}$, between oxygen atoms of different water molecules we use Toukan's Lennard-Jones potential

$$E_p = -\left(\frac{A}{r}\right)^6 + \left(\frac{B}{r}\right)^{12}, \tag{15}$$

with the constants $A = 0.371\,22$ nm $(\text{K J mol}^{-1})^{1/6}$ and $B = 0.3628$ nm $(\text{K J mol}^{-1})^{1/12}$, which they obtained in their study (see Fig. 2). The smaller intramolecular contributions to the potential energy (from the O-H and H-H vibrations) were omitted in this first round of simulations. Toukan and Rahman's model was based on a flexible rotating water molecule, and we use their approach to give us an extra parameter to model the absorption dip. The equivalent of the kinetic energy in the Fermi-Dirac distribution is given by the $h\omega$ term in the exponent. Assuming that most of this kinetic energy is coming from the rotation of the water molecule we obtain

$$\frac{m\omega^2 r(\omega)}{2} = \hbar\omega. \tag{16}$$

The distance $r(\omega)$ is a frequency-dependent parameter which allows us to modify the behavior of the imaginary refractive index in region 2. The distance r is the same as in the potential energy equation (15), Fig. 2. The final expressions for our fitting expression as a function of frequency can then be written as

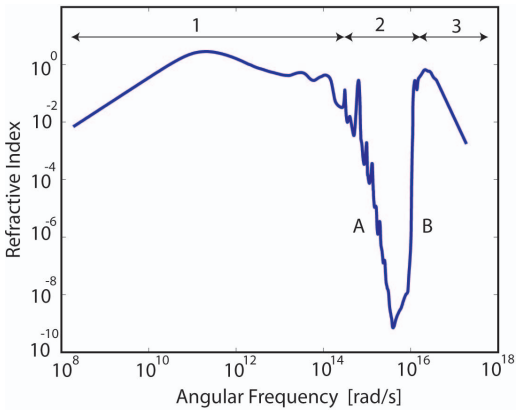

FIG. 1. (Color online) Different regions of the imaginary refractive index for water.

$$a_i(\omega) = \sum_{i=1}^{M} \frac{\sum_{\ell=0}^{n_i} N_{i,\ell}\omega^\ell}{\sum_{\ell=0}^{d_i} D_{i,\ell}\omega^\ell}, \tag{17}$$

$$b(\omega) = \sqrt{\frac{\chi_0}{1 + e^{\hbar\omega/(3/2kT) - E_p(\omega)}}\left[1 - \frac{1}{\ln(\tau_2/\tau_1)}\right]\ln\frac{i\omega\tau_2 + 1}{i\omega\tau_1 + 1}} + \sqrt{\varepsilon_\infty - \frac{\omega_0^2(\varepsilon_0 - \varepsilon_\infty)}{\omega^2 - \omega_0^2 - i2\gamma\omega}\frac{1}{1 + e^{\hbar\omega/(3/2kT) - E_p(\omega)}}}, \tag{18}$$

$$E_p(\omega) = \left(\frac{2\hbar}{m\omega}\right)^6\left[B^{12}\left(\frac{2\hbar}{m\omega}\right)^6 - A^6\right]. \tag{19}$$

III. SIMULATIONS IN WATER

As mentioned earlier, the double sum in Eq. (8) is performed near the resonances in regions 1, and 2*A*, and 2*B*,

TABLE I. Resonance frequencies used for the fractional dielectric function.

Frequencies	rad/s
ω_1	1.9×10^{13}
ω_2	9.4×10^{13}
ω_3	1.9×10^{14}
ω_4	4.4×10^{14}
ω_5	6.0×10^{14}
ω_6	1.3×10^{15}
ω_7	5.0×10^{15}
ω_8	1.3×10^{16}

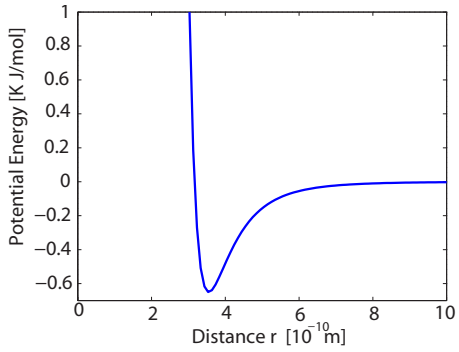

FIG. 2. (Color online) Energy potential for the oxygen-oxygen interaction based on the Lennard-Jones potential in Eq. (15) as derived by Toukan and Rahman [22].

Fig. 1. The general formula uses M resonances which for our water simulations is set to the value $M=8$. The resonances we used are shown in Table I (see also Fig. 3). Resonance 1 is from librational modes in the water, resonances 2–7 are from different combinations of stretching and bending modes, and resonance 8 is an electronic transition [27]. For each of these resonances we adopted a fractional form for describing the refractive index, Eq. (9). The different n_i and d_i ranged between 1–5 and 6–14, respectively, depending on the resonance; i.e., different resonances converged with different speeds towards the experimental data. This approach gives a reasonable fit to the real refractive index over the 10^8-10^{16}-Hz region and for the imaginary refractive index, except in the visible window. Introducing the $b(\omega)$ function and using the distance $r(\omega)$ between the adjacent oxygen atoms as our key fitting parameter, we are able to adjust our formula to the visible window in the imaginary part. In Fig. 4, we plot the functional dependence of $r(\omega)$ in the frequency regime 10^8-10^{16} Hz required to optimize the fit to experimental data. A distance of $r\approx 3$ Å is determined for the minimum value of the imaginary part of the refractive index, which compares well with the minimum energy based on Toukan and Rahman's Lennard-Jones potential. The needed variation of r, for different frequencies, to optimize the fitting process is physically reasonable since it describes the

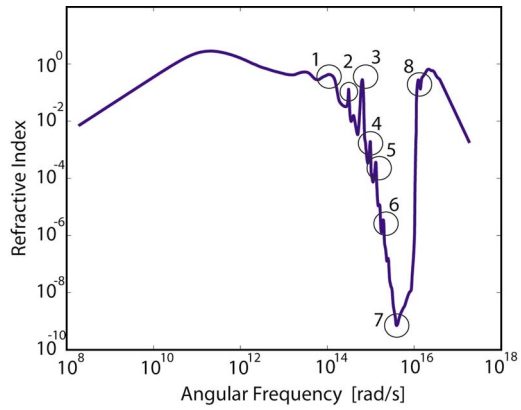

FIG. 3. (Color online) Resonances used for fitting procedure.

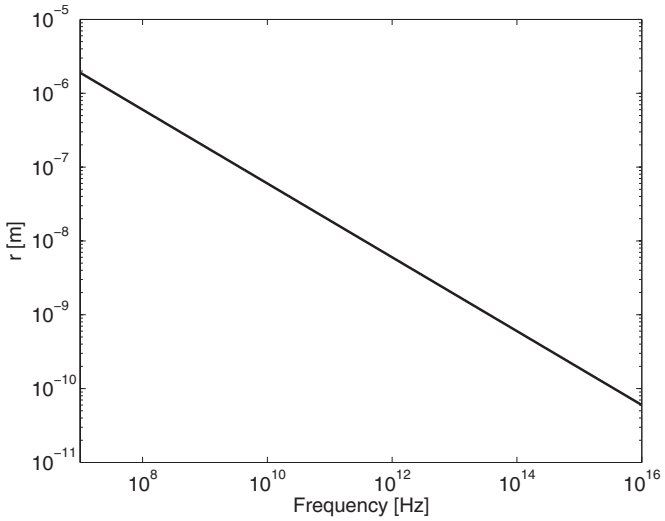

FIG. 4. Variations of $r(\omega)$ with frequency for obtaining optimum fit to data.

natural water network vibrations. Our final result for fitting the real and imaginary parts of the refractive index to measured data is shown in Figs. 5 and 6. The fitted parameter values used for the plots in Figs. 5 and 6 are not printed due to the large number; however, they may be retrieved from our website [28] together with the complete MATLAB code used for the fitting procedure.

Visual inspection of the curves suggest that the fitting procedure is quite successful. To obtain a more quantitative measure of the difference between model and measured data we use the error analysis described by Liebe *et al.* [29]. We calculate the absolute magnitude of the residuals $\delta_{re}=|\mathrm{Re}(n_{data}-n_{model})|$ and $\delta_{imag}=|\mathrm{Im}(n_{data}-n_{model})|$, respectively, Figs. 7 and 8.

We observe, from Figs. 7 and 8, that the residual for the real part of the refractive index is smaller than 10% for all frequencies except around 5×10^9 Hz and 5×10^{14} Hz where

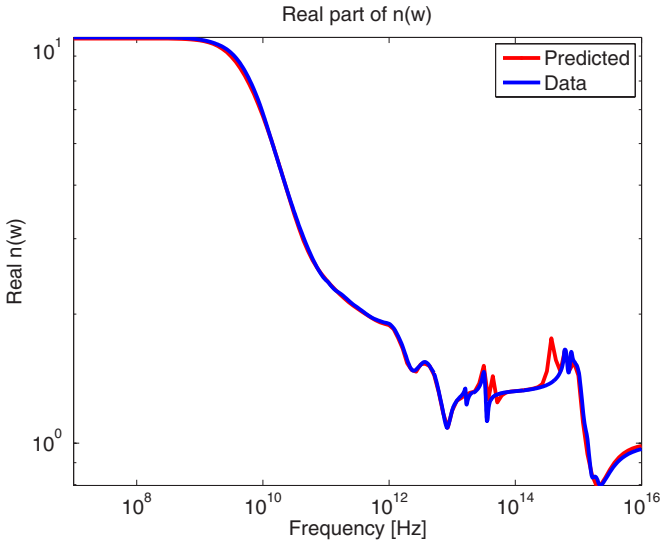

FIG. 5. (Color online) Real refractive index.

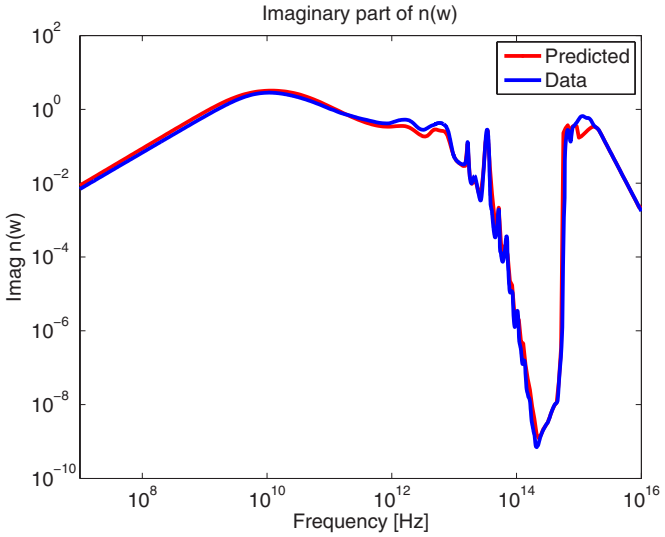

FIG. 6. (Color online) Imaginary refractive index.

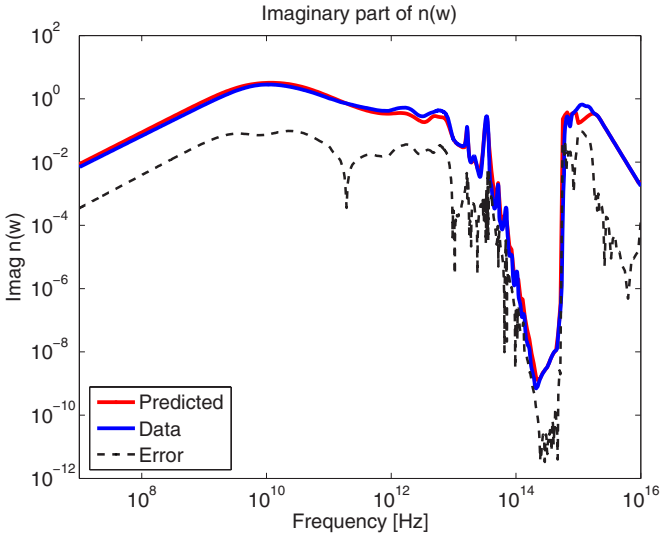

FIG. 8. (Color online) Absolute magnitude of the residuals for the imaginary refractive index.

the error is slightly larger than 10%. For the imaginary part of the refractive index the residual is always smaller than 1%. These relatively small residuals should not be unduly stressed since the experimental data have significant, and in some cases undocumented, errors associated with them—e.g., [30] (see Fig. 9).

For completeness, we are taking the Fourier transform of the fitted refractive index to obtain, graphically, the time dependence of the refractive index. It is observed that the water has several time constants ranging between femtoseconds and microseconds. However, since our fitting procedure is based on experimental data with 1–3 Å wavelength resolution it is unclear what information can be concluded for time periods larger than approximately 1 ps.

IV. DISCUSSION AND CONCLUSION

Using a combination of a fractional form for the dielectric function and a statistical physics approach to modeling intramolecular interactions, we have derived a phenomenological formula for the refractive index of water over the frequency region 10^8–10^{16} Hz. Using the model-based parameter estimation algorithm we have fitted our formula to the experimental data with better than 1 part in 10 accuracy including the visible window in the imaginary part of the refractive index.

Note that for any *small subset* (except for the visible window) of the frequency region 10^8–10^{16} Hz it is possible, with our formula or with others, to perform a more accurate fit than the one seen in Figs. 5 and 6. For example, in themicrowave region one could use the Rocard-Powles function to

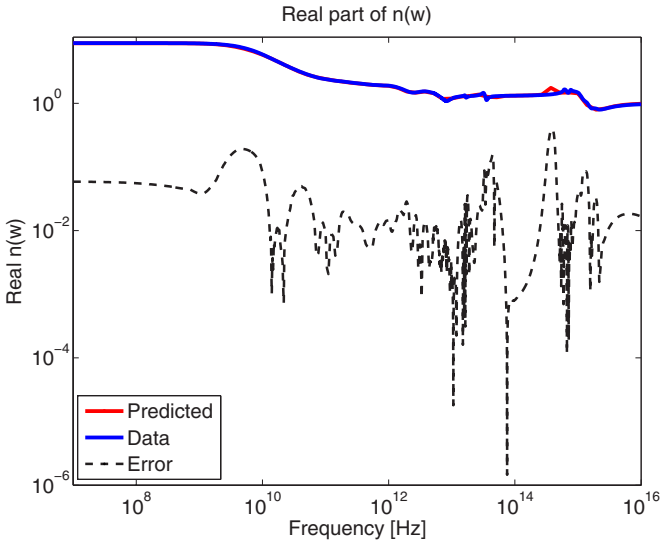

FIG. 7. (Color online) Absolute magnitude of the residuals for the real refractive index.

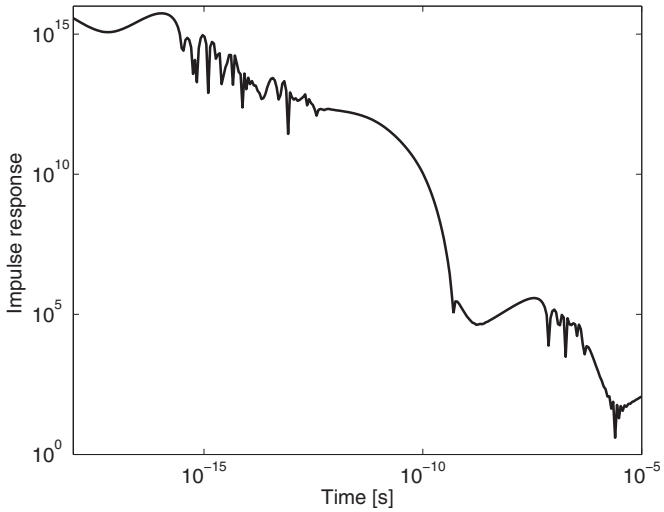

FIG. 9. The temporal evolution of the fitted refractive index for water.

obtain a more accurate fit than ours. However, for studies requiring an analytic formula for water's permittivity over a large frequency range including the visible window we believe that our formula is the most accurate to date.

ACKNOWLEDGMENTS

This work was partially funded by NIST, Grant No. 60NANB4D1142.

[1] http://omlc.ogi.edu/spectra/water/abs/ and http://www.martin.chaplin.btinternet.co.uk/index2.html
[2] R. R. Dagastine, D. C. Prieve, and L. R. White, J. Colloid Interface Sci. **231**, 351 (2000).
[3] J. E. K. Laurens and K. E. Oughstun, in *Ultra-Wideband, Short-Pulse Electromagnetics 4*, edited by E. Heyman (Kluwer Academic, New York, 1999).
[4] S. H. Choi and U. Österberg, Phys. Rev. Lett. **92**, 193903 (2004).
[5] U. J. Gibson and U. Österberg, Opt. Express **13**, 2105 (2005).
[6] R. R. Alfano, J. L. Birman, X. Ni, M. Alrubaiee, and B. B. Das, Phys. Rev. Lett. **94**, 239401 (2005).
[7] K. E. Oughstun, IEEE Trans. Antennas Propag. **53**, 1582 (2005).
[8] T. M. Roberts, Phys. Rev. Lett. **93**, 269401 (2004).
[9] X. Ni and R. R. Alfano, Opt. Express **14**, 4188 (2006).
[10] A. E. Fox and U. Österberg, Opt. Express **14**, 3688 (2006).
[11] K. E. Oughstun and G. C. Sherman, *Electromagnetic Pulse Propagation in Causal Dielectrics* (Springer-Verlag, Berlin, 1994).
[12] S. Rikte (unpublished).
[13] A. B. Djurisić and B. V. Stanić, Appl. Opt. **37**, 2696 (1998).
[14] R. E. Díaz and N. G. Alexopoulos, IEEE Trans. Antennas Propag. **45**, 1602 (1997).
[15] Y. Zubavicus and M. Grunze, Science **304**, 974 (2004).
[16] S. Woutersen, Ph.D. thesis, University of Amsterdam, 1999.
[17] P. H. Hahn, W. G. Schmidt, K. Seino, M. Preuss, F. Bechstedt, and J. Bernholc, Phys. Rev. Lett. **94**, 037404 (2005).
[18] D. W. Berreman and F. C. Unterwald, Phys. Rev. **174**, 791 (1968).
[19] J. L. Ribeiro and L. G. Vieira, Eur. Phys. J. B **36**, 21 (2003).
[20] A. von Hippel, *Dielectrics and Waves* (Wiley, New York, 1954).
[21] D. J. Segelstein, M.Sc. thesis, University of Missouri-Kansas City, 1981.
[22] K. Toukan and A. Rahman, Phys. Rev. B **31**, 2643 (1985).
[23] E. K. Miller, IEEE Trans. Antennas Propag. **40**, 42 (1998).
[24] C. L. Braun and S. N. Smirnov, J. Chem. Educ. **70**, 612 (1993).
[25] W. F. Chan, G. Cooper, and C. E. Brion, Chem. Phys. **178**, 387 (1993).
[26] O. Madelung, *Introduction to Solid-State Theory* (Springer-Verlag, Berlin, 1987).
[27] http://www.martin.chaplin.btinternet.co.uk/index2.html
[28] https://www.dartmouth.edu/ulfo/New_index.html
[29] H. J. Liebe, G. A. Huffard, and T. Manabe, Int. J. Infrared Millim. Waves **12**, 659 (1991).
[30] R. A. J. Litjens, T. I. Quickenden, and C. G. Freeman, Appl. Opt. **38**, 1216 (1999).